CHAPTER 1

Introduction

1.1 Role of fuselage frames in energy absorption

Crashworthiness is an important concern in vehicle structural design. The goal of crashworthy vehicle design is to increase occupant survivability and reduce the severity of injuries in crashes, and the most important contributor to this goal in the structural design is to limit occupant accelerations to survivable levels. Limiting occupant accelerations is achieved by designing the vehicle structure to absorb as much of the crash impact energy as possible. Impact energy is absorbed by progressive failures of the structure, and controlling the occurrence and sequence of these failures is the key to achieving optimal crash energy absorption. The main design requirements for maximizing crashworthiness in structures (Woodson, 1994) are:

1. maximizing the capacity of the structure to absorb impact energy, and

2. limiting the magnitude of the peak accelerations to human survivable levels.

The subject motivating this work is the crashworthiness of large transport aircraft. As discussed by Woodson (1994), the typical survivable crash for a transport category aircraft occurs near the airport at flight velocities of 150 knots, and a vertical descent rate of less than twenty-one feet per second. The horizontal component of the aircraft's speed at impact results in sliding of the aircraft forward along the ground, assuming no contact with a barrier. Consequently, the horizontal component of the speed at impact decreases to

zero more slowly than the vertical component of the speed at impact. Large vertical decelerations result from the rapid decrease in the vertical component of speed, and it is the vertical descent rate that is of interest here. For large transport aircraft, the vertical impact forces felt at the main passenger deck can be mitigated by stroking of the landing gear, crushing of the fuselage structure below the deck, and by stroking of the seat support structure. We are concerned with the role of crushing of the fuselage structure below the main passenger deck in absorbing the impact energy.

1.1.1 Fuselage drop tests

Drop testing of fuselage structure is a common method to study how the energy is absorbed by the structure due to the vertical component of the impact velocity. For example, Carden et al. (1990) report on a systematic series of tests and analyses of increasingly complex composite fuselage substructures under vertical drop testing to understand the response of the substructure under crash-type loads. The sequence of structures consisted of individual fuselage frames, a skeleton sub-floor structure of frames and stringers without the skin, and finally the stiffened sub-floor structure including the covering skin. The similarity in the fundamental response and failure of these substructures was shown to be governed largely by the frame, and composite fuselage frames are predisposed to fail by brittle fracture under crash-type loads. It was also observed that composite frames fracture across their entire cross-section at nearly the same circumferential locations under both static and dynamic test conditions. The first fractures normally occur at the load contact point with subsequent fractures occurring at approximately 45 to 50 degrees on either side of the contact point. Large frame segments that effectively brake free during the failure process are isolated from the main load path. Energy absorption is lowered because less material is involved in the failure process. In contrast, aluminum fuselage frames tend to maintain structural integrity of the load path during failure through the process of yielding and ductile folding. Maintaining or improving upon the existing levels of crashworthiness exhibited by conventional aluminum fuselage structures is an important criterion for composite fuselage structures, since poor crashworthiness would adversely affect their widespread use and acceptance.

1.1.2 Frame tests and analyses

Since the static and dynamic (for survivable crash speeds) failure sequences are nearly the same, and the frames play a central role in the crushing response of the fuselage substructure, the focus of the present study is on the static response of individual frames. Actually, the present study is a continuation of the work by Moas et al. (1994), Woodson (1994), and Woodson et al. (1996). The Moas et al. study consisted of tests and analyses of semi-circular, I-section frames, six-feet in diameter, fabricated from graphite/epoxy unidirectional tape. Woodson (1994) developed an analysis and design algorithm to optimized composite material frames under static crush-type loads. The objective of the optimal design algorithm is to maximize the energy absorbed subject to a constraint on the maximum load. This is objective is illustrated in Fig. 1.1, in which a comparison between two possible scenarios in a fuselage drop test is shown. In this figure, idealized plots of the vertical contact force versus the vertical displacement due to crushing of the structure below the passenger deck are depicted. The area under the force-displacement response curve represents the energy absorbed due to crushing of the structure. The design with low peak acceleration force and high energy absorption is the one preferred in crashworthy design. So, maximizing the crashworthiness of a structure is equivalent to maximizing the area under the load-displacement response curve of a structure, subject to a constraint on the maximum failure load.

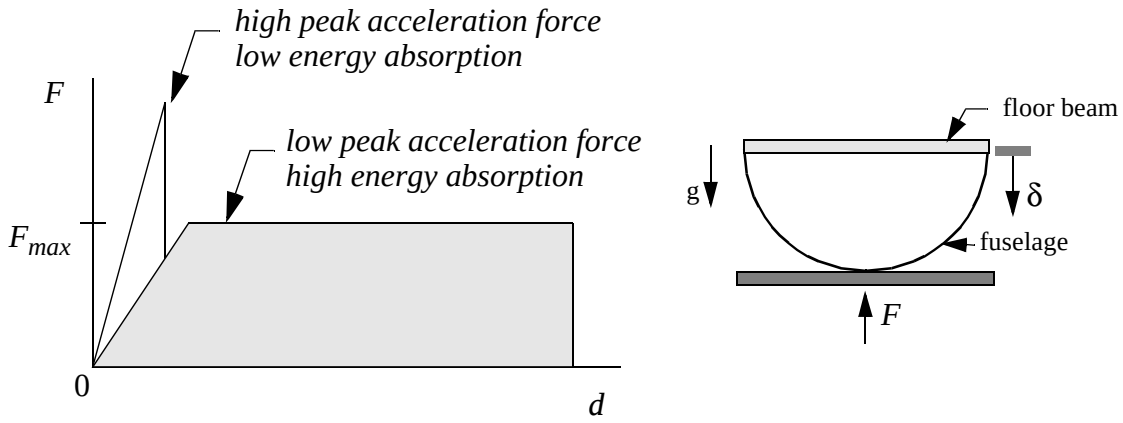

Fig. 1.1 Possible energy absorption scenarios.

The first part of this study concerns tests, analyses, and optimizations of the frames laminated from graphite-epoxy unidirectional tape that remained from the Moas et al. (1994) study. A detailed description of these tape layup frames is presented in Section 1.2. Moreover, we have available circular frame segments with a 118-inch inner radius, 102 inches long, and manufactured using textile composite preforms and a resin transfer molding process. In the second part of this study, we report on the static tests of textile frames. A description of these textile frames is presented in Section 1.3.

1.2 Tape layup composite frames

Static tests of the semicircular, six-foot diameter, I-section frames are conducted in a universal testing machine both in the study by Moas et al. (1994) and in this study. The ends of the specimens are secured to a steel I-beam and the steel I-beam is in turn attached to the fixed cross head of the testing machine. The bottom of the frame contacted the movable table of the testing machine, and the table is displaced at a constant rate to initially load the specimen at approximately 1000 lbs per minute. To clamp the ends of the frame to the steel beam (Fig. 1.2) slots in the shape of the I-section are machined into two steel blocks, with the slots about 0.2 inches wider than the thickness of the flanges and web of the specimen. The ends of the specimen are secured in the slots of the blocks using a potting material. A schematic of the test is shown in Fig. 1.2 and the cross section of a typical frame is shown in Fig. 1.3. These frames are fabricated from graphite-epoxy unidirectional tape. The cross-section is constructed using two channel sections co-cured with cap plies and skin plies, as shown in Fig. 1.4 (Moas et al., 1994). The channel sections are formed by wrapping the plies around a semicircular tool; the cap plies are then added to the top and bottom of the channels, forming the inboard and outboard flanges, respectively. A cylindrical skin is co-cured to the radially outboard flange of the frame providing lateral stiffness to the frame-and-skin structure. Increased lateral stiffness keeps deformations in the plane of the frame in order to realistically represent deformations as they occur in a actual fuselage structure. The stacking sequence in the web and flanges, the web height, and the radius of each frame are listed in Table 1.1.

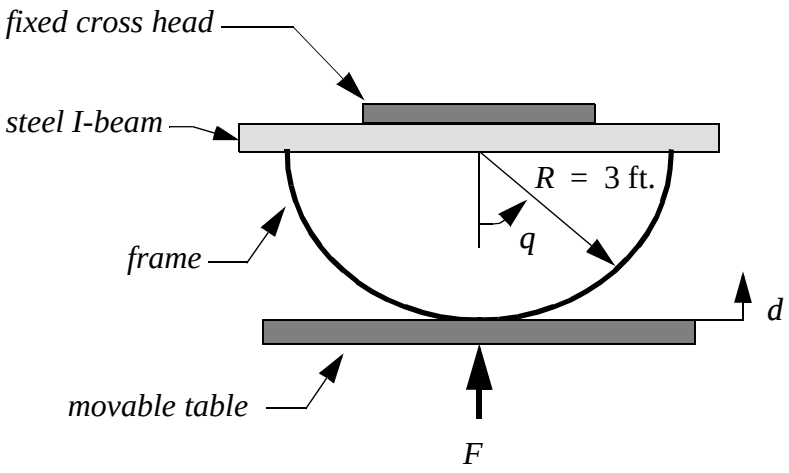

Fig. 1.2 Schematic of the semicircular frame test.

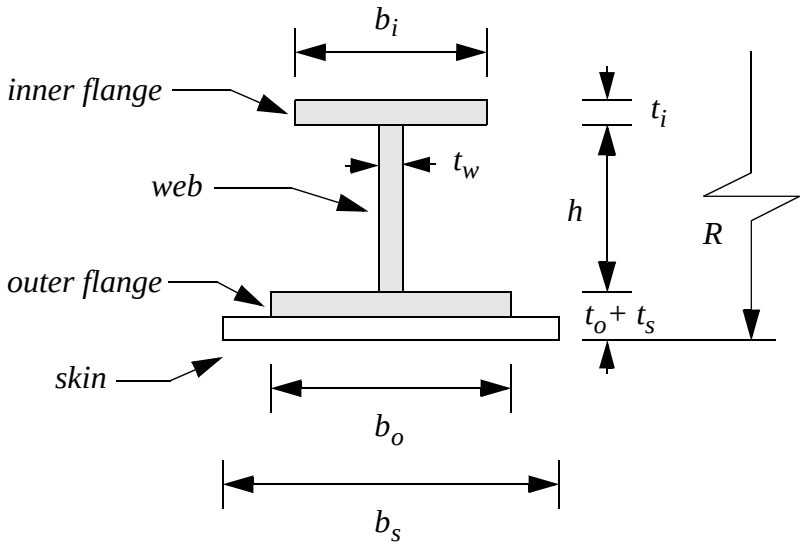

Fig. 1.3 Cross-section of the I-section frame showing skin bonded to the outer flange.

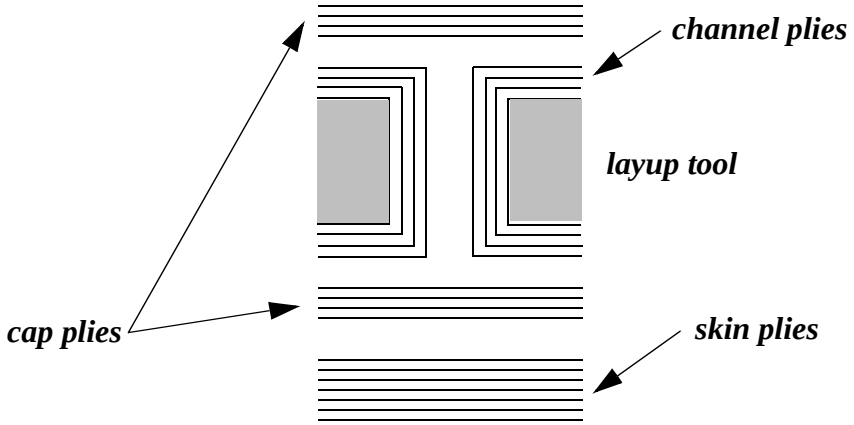

Fig. 1.4 Fabrication technique for frame cross-section (Moas et al., 1994).

Table 1.1 Semicircular I-section frame specimens[a].

frame label	serial number	stacking sequence flange	stacking sequence web	web height *h*, in.	radius *R*, in.
FR001I	1, 2, 3	$[\pm 45/0/90]_S$	$[\pm 45/0/90_2/0/-45/45]$	1.25	36.0
FR002I	1, 2, 3	$[\pm 45/0/90_2/0/-45/45]_S$	$[\pm 45/0/90_2/0/-45/45/-45/45/0/90_2/0/\pm 45]$	1.25	36.0
FR003I	1, 2, 3	$[\pm 45/-45/45/90/0_3]_S$	$[\pm 45/-45/45/90/0_6/90/-45/45/\pm 45]$	1.25	36.0
FR004I	1, 2	$[\pm 45/0/90]_S$	$[\pm 45/0/90_2/0/-45/45]$	0.75	36.0
FR005I	1, 2	$[\pm 45/0/90_2/0/-45/45]_S$	$[\pm 45/0/90_2/0/-45/45/-45/45/0/90_2/0/\pm 45]$	0.75	36.0
FR005I	1, 2	$[\pm 45/-45/45/90/0_3]_S$	$[\pm 45/-45/45/90/0_6/90/-45/45/\pm 45]$	0.75	36.0

a. The stacking sequence of the skin bonded to each frame is $[\pm 45/0/90]_{2S}$

Of the fifteen specimens listed in Table 1.1, Moas et al. (1994) reported on the tests of five frame/skin specimens. A typical load-displacement response (*F*-*d* plot) from the tests exhibits a large drop in the load after the first major failure event, which is not the ideal response from a crashworthiness perspective. (Refer to Fig. 1.1.) Four of the specimens left untested from Moas et al. (1994) are tested as part of this research, and these frames

along with the average value of their measured dimensions are shown in Table 1.2. Three

Table 1.2 Average measured dimensions of selected semicircular frames.

frame	thickness skin, in.	thickness outer flange, in.	thickness web, in.	thickness inner flange, in.	web height, in.	radius, in.
FR002I-1	0.0834	0.0778	0.0814	0.0851	1.247	36.067
FR002I-3[a]	0.0830	0.0780	0.0810	0.0840	1.251	36.094
FR005I-2	0.0831	0.0824	0.0830	0.0863	0.748	35.844
FR006I-1[a]	0.0840	0.0820	0.0810	0.0830	0.748	36.407
FR006I-2	0.0850	0.0830	0.0841	0.0841	0.748	35.577

a. Moas (1996)

of these frames were redesigned using the analysis and design computer code developed by Woodson (1994). This design and analysis code has the capability to design both the geometry and laminate stacking sequence to improve the crashworthy response, as is described in the next chapter. However, for the existing frames from Moas et al. (1994), we could only reduce the flange widths to improve the response, so the analysis only considered the width of the flanges as the design variables. Hence, one of the purposes of this research is to present the test results of three, redesigned I-section frames in order to assess the design and analysis methodology used by Woodson (1994). These results were previously presented in Pérez et al. (1998).

The coordinate system, displacements, and rotations used by Woodson (1994) for the semicircular frame are illustrated in Fig. 1.5. The displacements and rotations of material points on the reference arc are referred to cylindrical coordinates. Let q denote the polar angle, $-\pi/2 < q < \pi/2$, and let R denote the radius of the reference circular arc. The displacements (U, V, W) and rotations (F_x, F_y, F_z) are defined on the reference arc of the frame, and are functions of the polar angle only. The circumferential displacement is denoted by U, the out-of-plane displacement by V, the radially inward displacement by W, the angle of twist by F_x, the rotation angle for in-plane bending by F_y, and the rotation for out-of-plane bending is denoted by F_z.

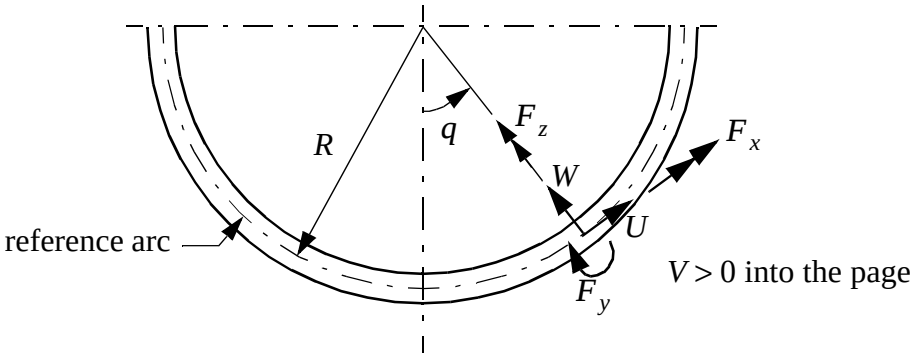

Fig. 1.5 Displacement and rotations of the semicircular frame.

1.3 Textile composite frames

The five textile composite frames available for this research were supplied to the NASA Langley Research Center under NASA Contract NAS1-19348 (Structures and Material Technologies for Aircraft Composite Primary Structures) by the Lockheed Aeronautical Systems Company. These frames were specified by NASA to be J-sections with a 118-inch inner mold line radius, a length of 102 inches, and a maximum depth of 4.8 inches. The attached, or faying, flanges are machined to include a 20° edge taper. The cross-section and nominal dimensions of a typical frame delivered to the Langley Research Center are shown in Figure 1.6. Appropriate thicknesses were specified to be sufficient to achieve load capability as follows: 55,000 lb-in. (skin in tension) with 2463 lb axial tension, and -38,887 lb-in. with 4470 lb axial tension. Detailed measurements of each frame, as well as other engineering data for these frames, are presented in Chapter 4. The coordinate system, displacements, and rotations used for these frames are illustrated in Fig. 1.7.

The frames were manufactured at Lockheed's facility in Marietta, Georgia by resin transfer molding using 3M PR500 epoxy resin into a textile preform made of AS-4 carbon fiber (Barrie and Skolnik, 1993; Jackson, 1994). The preforms are nominally 0°/± 60°, 2D triaxial braid construction with a fiber volume specified to be 58% ± 3% for the cured component. The braid architecture is $18k_{axial}/6k_{bias}$ (Barrie and Skolnik, 1993; Jackson,

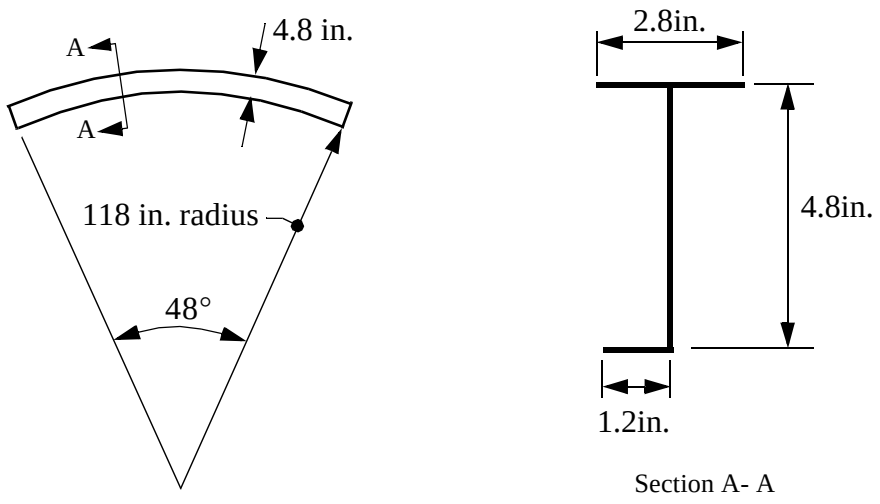

Fig. 1.6 Nominal dimensions of the textile composite J-section frames.

1994). A detailed description of braided textile materials is given in Section 1.3.2 on page 11. However, we first discuss the general class of textile composite materials in the following section.

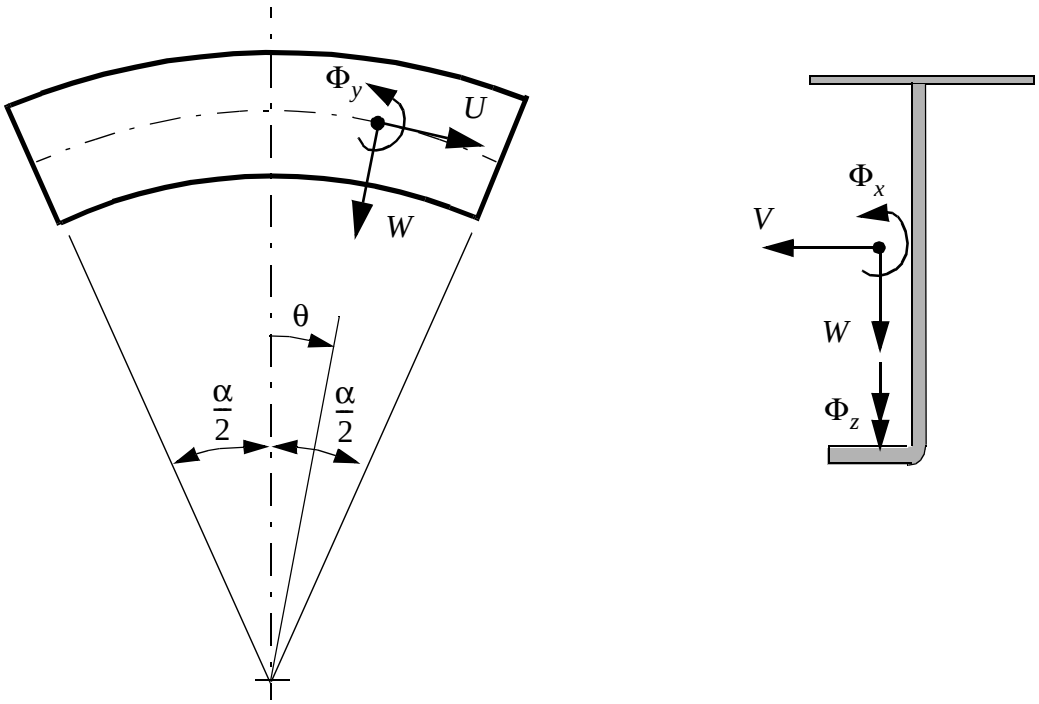

Fig. 1.7 Textile composites J-section frames displacements and rotations.

1.3.1 Textile composite materials

Textile structural composites are a type of advanced composite containing fiber preforms produced by textile forming techniques such as weaving, braiding or knitting of the fiber yarns. This class of composites is composed of a textile fiber, yarn, or fiber system, as well as resin, metal, or ceramic components (Chou, 1992). The increased interest in these composites arise from the need for improvements in through-the-thickness strength and damage tolerance with respect to tape laminates. They also have the unique capability that the fabric preforms can be fabricated directly to their final shapes or can be machined to specified contours and dimensions; that is, textile composites offer cost savings from increased automation in manufacturing. Also, textile composites are superior to other materials on a strength-to-weight and stiffness-to-weight basis, making them especially suitable for structures where weight saving is an important issue. The fiber architecture of a textile composite is very complex, so many parameters control its mechanical properties.

Yarns are linear assemblages of fibers formed into continuous strands having textile characteristics of substantial strength and flexibility. Textile structural composites are made from high modulus fibers or yarns. Currently, the most commonly used types of high modulus yarns are composed of glass, graphite, aramid, ceramic, and steel fibers. For aircraft, rockets, and other applications where stiffness-to-weight and strength-to-weight are major considerations, graphite has become the most commonly used material (Chou, 1992). The relative density of fiber packing in the yarn cross-section is quantified by the fiber packing fraction, which is the ratio of fiber specific volume to yarn specific volume. Fiber packing fractions are determined by a number of factors, including the number of fibers in a yarn, fiber cross-sectional shape, yarn tension, level of yarn twist, and yarn manufacturing method (Chou, 1992).

The primary function of the resin system is to provide rigidity and to hold the textile reinforcement material (fibers, yarns, or fabrics). The resin system provides rigidity and stability to the textile composite.

The assemblage of fibrous materials (fibers, yarns, or fabrics) is known as the textile composite preform. To form a continuous material, the resin is applied to the textile pre-

form and must penetrate all the interstices and wet all of the exposed fiber surfaces throughout the textile preform. No air bubbles should be entrapped permanently within the composite, so resin impregnated textile preforms are exposed to high pressures during the forming, shaping and molding processes necessary to produce the textile composite.

1.3.2 Triaxial braided composite materials

Braiding is a textile process in which two or more systems of yarns are intertwined diagonally to form an integrated structure. Braided preforms are fabricated over a mandrel to the desired thickness. This is achieved by over braiding layers. A single layer of a 2D braid consist of either two or three intertwined yarns. The braider yarns follow the $+q_b°$ and $-q_b°$ directions and usually interlace in either a 1x1 or a 2x2 pattern. A 1x1 pattern (Fig. 1.8) is similar to the interlacing in a plain weave fabric (Fig. 1.9). In a 2x2 pattern a

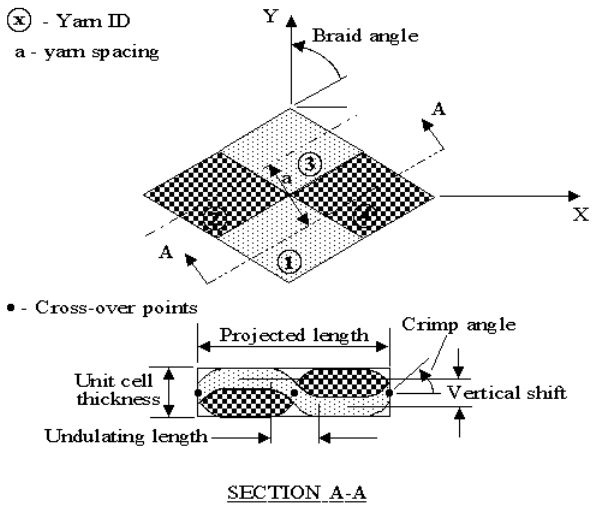

Fig. 1.8 Unit cell for a 2D braid (Naik, 1994c).

$+q_b°$ braider yarn continuously passes over two $-q_b°$ braider yarns and then under two $-q_b°$ braider yarns and vice versa. A 2D triaxial braid consist of axial yarns in addition to the off-axis braider yarns (Fig. 1.10). The axial yarns follow the longitudinal direction and are inserted between the braider yarns. They are incorporated into the fabric during braiding through stationary guide tubes (Suherman, 1996). They are inserted between the

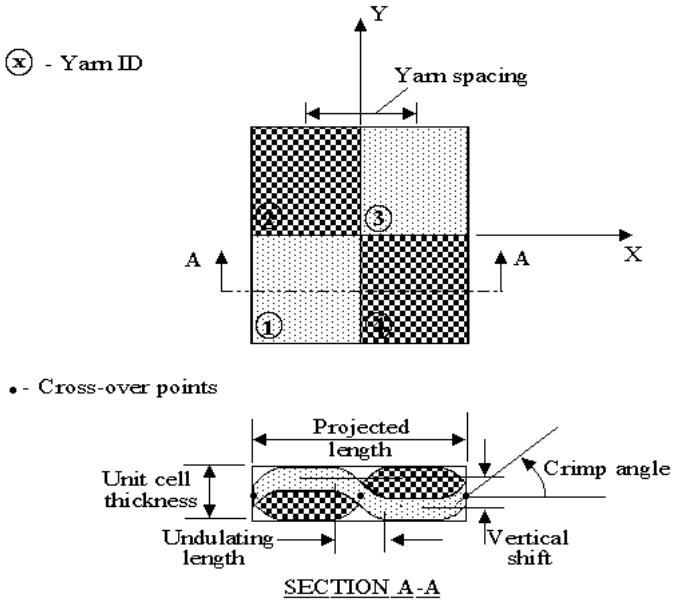

Fig. 1.9 Unit cell model for a plain weave composite (Naik, 1994c).

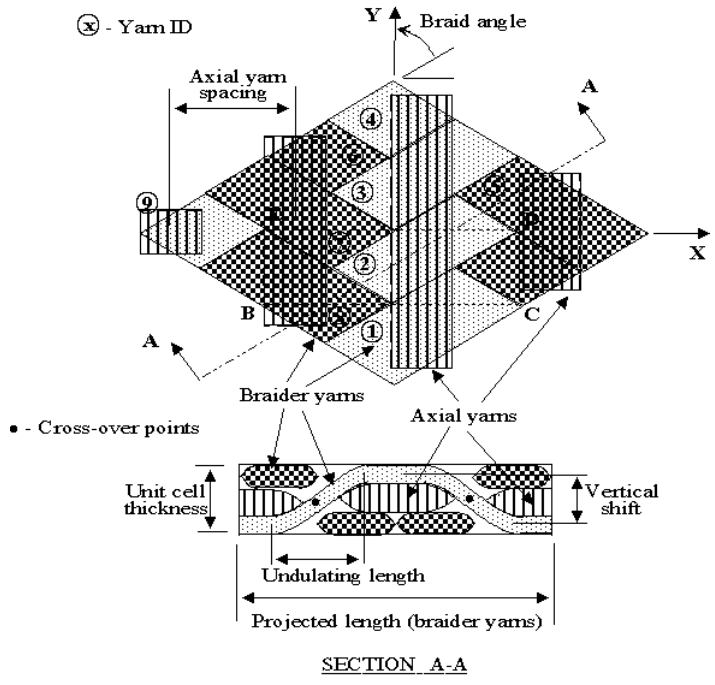

Fig. 1.10 Unit cell for a 2x2 2D triaxial braid (Naik, 1994c).

braided yarns and are not truly intertwined with the bias yarns. These yarns are parallel to the braid axis and are supposed to be straight (without crimp).

A 2D braided composite laminate of a certain desired thickness is formed by over braiding layers of the desired architecture on top of each other. After the preform is removed from the mandrel, slit along the axial direction, flattened and border stitched, resin is introduced by a resin transfer molding process. This leads to a 2D material since there are no interlayer yarns through the laminate thickness.

In 2x2 2D triaxial braided composite materials three of the most important braid parameters are braid angle, yarn size (measured in *k*, where 1*k* equals 1000 filaments), and volumetric proportion of axial (0°) yarns to total yarn content, which is a function of the first two parameters. Yarn size is expressed in terms of the number of filaments per yarn. The unit cell dimensions vary considerably and are in general relatively large. The unit cell width is defined as twice the spacing of the axial yarns, while the unit cell length is twice the distance, along an axial yarn, between the intersections of an axial yarn and a $+q_b°$ braider yarns (these factors of 2 are due to the fact that this is a 2x2 pattern).

A shorthand notation, similar to the one used to define the stacking sequence of laminates formed of unidirectional pre-impregnated tape, has been introduced (Masters and Minguet, 1994) to define the braid architecture. It incorporates the three preform parameters listed above. The proposed notation is: $[0°_{x\mathrm{k}}/\pm q_b°_{y\mathrm{k}}]$ *N* % axial, where q_b indicates the braid angle, *x* indicates the number of fibers in the axial yarn bundles, *y* indicates the number of fibers in the braided yarn bundles, *k* indicates thousands, and *N* indicates the percentage by volume of axial yarns in the preform.

1.3.3 The TEXCAD computer code

The computer code TEXCAD (Textile Composite Analysis for Design), was developed by Naik (1994a, 1994b, 1994c, 1995, 1996) to analyze a wide variety of fiber reinforced woven and braided composites, including plain weave, 2D braided, 2D triaxial braided, and 3D braided composites. The micromechanics analysis employed in TEXCAD assumes an iso-strain state in a discrete model of the yarn structure within the textile

repeating unit cell (RUC). The code can compute effective thermal and mechanical properties of the RUC, damage initiation and progression, and strength of woven and braided composites. For the input to the code, the material parameters such as yarn size, braided angle, yarn crimp, and yarn spacing are needed. Overall effective stiffness properties computed by TEXCAD correlate well with test data over a wide range of architecture parameters (Naik et al., 1993). For braided composites, Naik found that the in-plane properties varied significantly with the braid angle, and the strength decreased with increasing the braid angle or the axial yarn crimp angle. Masters et al. (1995) used TEXCAD to examine the mechanical properties of 2D triaxial braided composites. A parametric study was conducted in two parametric categories, i.e., primary braid parameters (yarn size, braid angle, axial yarn content) and secondary braid parameters (axial yarn spacing, crimp angle, zero degree yarn crimp angle). They found that the stiffness properties were strongly influenced by the braid angle and axial yarn content, although they are more sensitive to variability in the former. Zhang et al. (1996) noted that the braid parameters were related to one another.

1.4 Objectives

There are two main objectives of this research which are as follows.

1. To assess the design optimization computer code OPTFAIL (Woodson, 1994) by using it to redesign three of the existing frames remaining from the study by Moas et al. (1994) for improved energy absorption.

2. To conduct static tests to failure of the 2x2 2D triaxial braided composite frames, accompanied by a preliminary analyses of these tests using the ABAQUS finite element code. The effective moduli are obtained from the TEXCAD computer code.

In regard to the first objective, the optimization is limited to reducing the flange widths around the circumference of the semicircular, I-section frames made from graphite-epoxy unidirectional tape, although the OPTFAIL code can include laminate stacking sequences as design variables as well. A fourth frame from the Moas study is tested in the as is condition to serve as a baseline test. The baseline test results are used to update the stiffness

parameters in the analysis module of OPTFAIL, and as benchmark to assess the performance of the redesigned frames. The analysis module of OPTFAIL is called PROFAIL.

In regard to second objective, a limited number of material characterization tests are performed on coupons of the 2x2 2D triaxial braided composite material cut from one of the braided frames. Moduli and strength data obtained from the tests are used to determine the textile material parameters input to the TEXCAD code that best fit the experimental data. Then the effective moduli determined by TEXCAD code are used as the material input data to the ABAQUS code for the prediction of overall frame response.

1.5 Organization of this document

The implementation and results of the computer code OPTFAIL to redesign the three semicircular frames made from graphite-epoxy tape are presented in Chapter 2. Then the results of the tests of the redesigned frames are presented, followed by comparison of these test results to the predictions of PROFAIL code. The tests, and the test results, of braided composite coupons are presented in Chapter 3. Comparison of the coupon test results with analytical predictions from computer code TEXCAD are discussed. In Chapter 4, the test apparatus and test procedures for the braided composite frame tests are presented. Results of the braided frame tests are presented in Chapter 5, including the discussion of the model used to predict the response of these tests. Chapter 6 includes concluding remarks and recommendations for further research. A brief manual to use the computer codes developed by Woodson is presented in Appendix 1. A sample run using the computer code TEXCAD is presented in Appendix 2.